

# Centrality and system size dependence of (multi-strange) hyperons at 40A and 158A GeV: A comparison between a binary collision and a Boltzmann+hydrodynamic hybrid model.

Hannah Petersen,<sup>1,2</sup> Michael Mitrovski,<sup>1,2</sup> Tim Schuster,<sup>1</sup> and Marcus Bleicher<sup>2</sup>

<sup>1</sup>*Frankfurt Institute for Advanced Studies (FIAS),  
Ruth-Moufang-Str. 1, D-60438 Frankfurt am Main, Germany*

<sup>2</sup>*Institut für Theoretische Physik, Goethe-Universität,  
Max-von-Laue-Str. 1, D-60438 Frankfurt am Main, Germany*  
(Dated: July 23, 2019)

We present results on the centrality and system size dependence of (multi-strange) hyperons in Pb+Pb collisions at 40A and 158A GeV from the Ultra-relativistic Quantum Molecular Dynamics (UrQMD-v2.3) model and a coupled Boltzmann+hydrodynamics calculation. The second approach is realized in a hybrid fashion based on UrQMD with an intermediate hydrodynamical evolution for the hot and dense stage of the collision. This implementation allows to compare microscopic transport calculations with hydrodynamic simulations to explore the transition from a system which is not fully thermalized like C+C or Si+Si collisions to supposedly fully thermalized systems as e.g. created in Pb+Pb reactions. The results from our calculation are compared to measurements of the (anti-) hyperon yields at midrapidity ( $|y| \leq 0.5$ ) performed by the NA49 and NA57 collaborations at 40A and 158A GeV. Furthermore, we present predictions for the centrality dependence of  $\Lambda$ ,  $\bar{\Lambda}$  and  $\Xi^-$  rapidity spectra and total multiplicities at 40A and 158A GeV.

PACS numbers: 25.75.Dw

The only possibility to study nuclear matter under extreme conditions (apart from cosmic objects), is to create hot and dense nuclear matter in the laboratory. This can be achieved by colliding nuclei, either by shooting accelerated ions at a stationary target, like at the Alternating Gradient Synchrotron (AGS) at the Brookhaven National Laboratory (BNL) or the CERN Super Proton Synchrotron (SPS), or by head-on collisions of two ion beams, like at the Relativistic Heavy Ion Collider (RHIC) at the BNL and the Large Hadron Collider (LHC) at CERN. In order to achieve a “macroscopic” volume of excited nuclear matter, very heavy nuclei such as lead (Pb) or gold (Au) are used. At high temperature and baryon density, nuclear matter is expected to melt into a state of free quarks and gluons, known as the Quark-Gluon-Plasma (QGP) [1, 2, 3].

The strange ( $s$ ) and anti-strange ( $\bar{s}$ ) quarks are a well suited diagnostic tool to investigate the properties of the matter created in such collisions, because they are not contained in the colliding nuclei, but are newly produced. At the end of the reaction they show up in strange hadrons in the final state. In [4, 5] the authors suggested almost 25 years ago that strange particle production is enhanced in the QGP with respect to a hadron gas. This enhancement can be quantified relative to a reaction where a transition to a QGP phase can not take place, as in p+p collisions where the system size is very small. The enhancement occurs because in the QGP different channels are responsible for strangeness production, leading to a strong reduction of the strangeness thermalization time as compared to the hadronic scenario. This is supported by the difference in threshold energies due to the fact that in a deconfined state, only the strange quarks have to be produced, rather than strange hadrons them-

TABLE I: The energy threshold to create strange hadrons in hadronic interactions.

Production reaction	$E_{\text{threshold}}$ (MeV)
$N + N \rightarrow \Lambda + K^+ + N$	$\approx 700$
$N + N \rightarrow N + N + \Lambda + \bar{\Lambda}$	$\approx 2200$
$N + N \rightarrow N + N + \Xi^- + \bar{\Xi}^+$	$\approx 4500$
$N + N \rightarrow N + N + \Omega^- + \bar{\Omega}^+$	$\approx 5200$

selves. In a QGP the strange quarks are produced in gluon fusion ( $gg \rightarrow s\bar{s}$ ) and light  $q\bar{q}$  pair annihilation ( $q\bar{q} \rightarrow s\bar{s}$ ) processes. The threshold energy required to create a pair of  $s\bar{s}$  quarks in the QGP is just the bare mass of the two strange quarks ( $E_{\text{threshold}} \approx 2m_s \approx 300$  MeV). Due to high temperatures involved in the QGP phase, the thermal production of  $s\bar{s}$  pairs is possible. A further source of enhanced  $s\bar{s}$  production comes from the process of Pauli blocking of light quarks. Therefore, as more and more light quarks are produced in the collision, they fill up the available energy levels and it becomes energetically favourable to create  $s\bar{s}$  pairs.

It is expected that the extra mechanisms for  $s\bar{s}$  production in a QGP should lead to a production rate which is 10 to 30 times higher than in a hadron gas, resulting in an equilibration of strangeness even in the short lifetime of the fireball. Therefore, it is assumed that the production of strange and anti-strange baryons at freeze-out will be enhanced, if the system passes through a deconfined phase, as compared to a system that remained in the hadron gas phase only.

Furthermore, strangeness is a good quantum number because it is conserved in strong interactions. Strange quarks (and therefore strange hadrons) decay via the

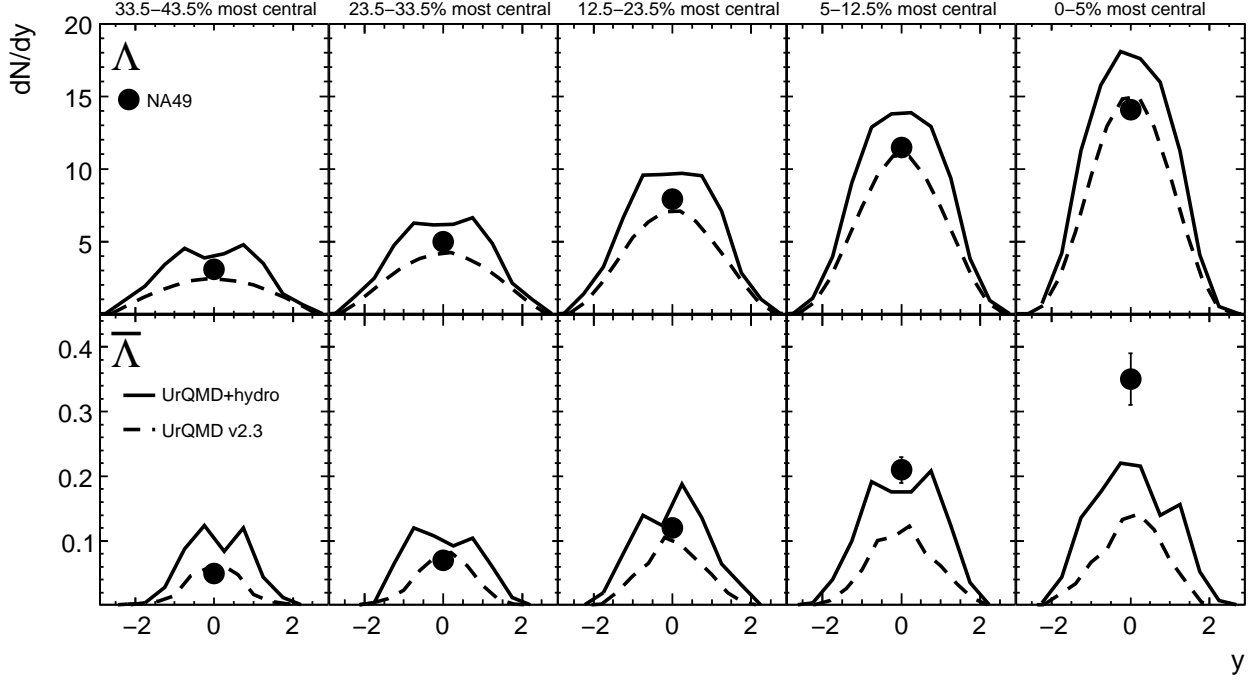


FIG. 1: The points correspond to the measured yield at midrapidity ( $|y| \leq 0.5$ ) for  $\Lambda$  (top) and  $\bar{\Lambda}$  (bottom) from NA49 [35, 36] measured for different centralities in Pb+Pb collisions at 40A GeV. The solid line represents calculations with UrQMD+hydro and the dashed line with UrQMD.

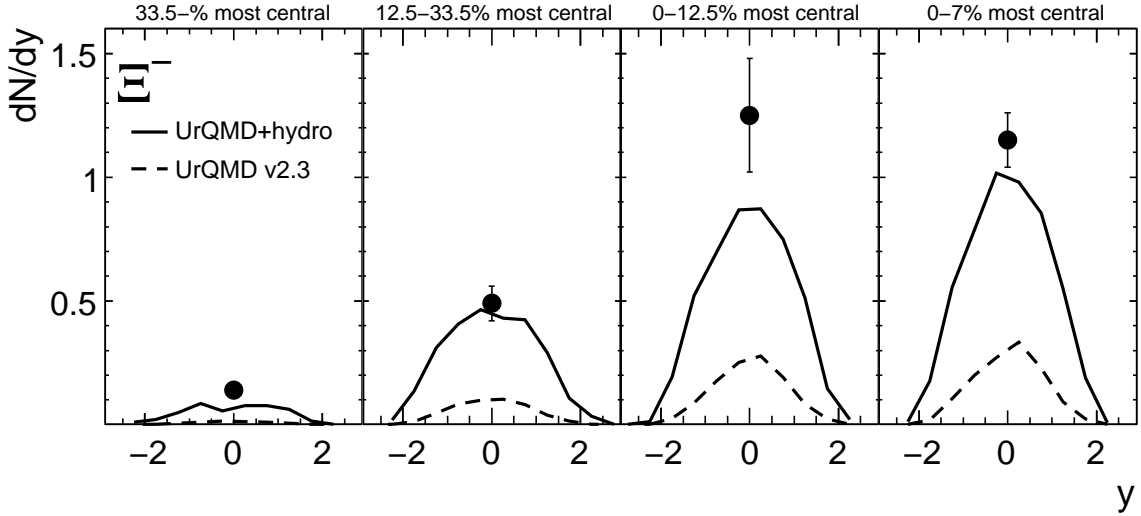


FIG. 2: The points correspond to the measured yield at midrapidity ( $|y| \leq 0.5$ ) for  $\Xi^-$  from NA49 [34, 35, 36] measured for different centralities in Pb+Pb collisions at 40A GeV. The solid line represents calculations with UrQMD+hydro and the dashed line with UrQMD.

weak interaction, where typical lifetimes are on the order of  $10^{-10}$  s and so these decays are not important on the time scale of a hadronizing QGP and can be well reconstructed by experiments.

To create strange hadrons in a hadronic interaction a high threshold energy is needed, which is calculated from

the differences in masses between the initial and the final state particles as shown in Table I for  $N+N \rightarrow$  (anti-) hyperons.

Because of these large threshold energies (multi-) strange baryon production through this channels is suppressed even in initial collisions in the SPS energy regime

( $\sqrt{s_{NN}} \approx 5\text{--}20$  GeV) [6, 7]. Important sources for (multi-strange) hyperon production are multi-step processes that lead to high mass resonance excitations and the rescatterings of initially produced anti-kaons. In regions of high net baryon density, also the production of strange baryons is more likely, especially  $\Lambda$ 's are produced in association with a kaon and this reaction has the lowest threshold energy of all hadronic processes to produce strangeness. In a hadron resonance gas it takes some time to equilibrate strangeness and the timescale of a heavy ion collision might be shorter than this equilibration time.

Different approaches to enhance strangeness production in semi-hadronic scenarios without a transition to a deconfined state have been proposed. In [8] a baryon junction exchange mechanism was proposed to explain valence baryon number transport in nuclear collisions and hence the production of (anti-) hyperons.

Another ansatz is the introduction of a strong color fields (color ropes) in string-hadronic models by a modification of the Schwinger mechanism [9]. When moving from  $e^+e^-$  or  $p+p$  interactions to heavy-ion collisions the string density can be so high that the color flux tubes are overlapping [10, 11, 12, 13]. Practically, this results in the non-independent fragmentation of QCD-flux tubes with higher color charge representation, e.g.  $\mathbf{8} - \bar{\mathbf{8}}$  strings instead of triplet charges. This implementation of the color electric field increases the production of hyperons.

Using multi-hadronic interactions can bring the system to local chemical equilibrium and enhance the production of anti-hyperons [14]. A similar way to push the system into chemical equilibrium is to imply multiple interactions of pions [15] or an oversaturation of the pion number [16]. Calculations in [17] showed that reaching an equilibrium in a pure hadronic medium, considering collision rates and time scales of the hadronic fireball expansion, is only possible if hadronic multi-particle interaction are taken into account. Recently, counter arguments against this conclusion were suggested within a hadronic Hagedorn model [18]. However, the main conclusion remains that close to the QGP phase boundary the densities are large and might drive the system quickly to a chemical equilibrium state.

The observed enhancement of strangeness can be explained also in statistical models by the transition from a canonical ensemble for small systems (e.g. like in  $p+p$ ), which treats charge conservation exactly, to a grand canonical ensemble for heavier systems like  $\text{Pb}+\text{Pb}$  or  $\text{Au}+\text{Au}$ . With this constraint the phase space for particle production is reduced in small systems. In order to compare this to experimental data, in [19], the correlation volume  $V$  of the system is proportional to  $\langle N_w \rangle$  for a constant center-of-mass energy ( $V = \frac{V_0}{2} \langle N_w \rangle$ , where  $V_0$  is the volume of the nucleon). An alternative approach to determine the correlation volume is suggested in the percolation model [20]. However, none of the above discussed approaches allows for a consistent description of both spectra and multiplicities of (multi-) strange baryons up to now.

strange baryons up to now.

In this paper we attack this question by using a hadronic transport approach, namely the Ultra-relativistic Quantum Molecular Dynamics (UrQMD) in version 2.3 [21, 22, 23] and compare the results to a hybrid approach where a hydrodynamic evolution is embedded into the model [24]. By doing this, we do not aim at the understanding of the dynamics of the strangeness equilibration process itself, but we are able to compare strangeness production in a full non-equilibrium approach with a dynamical approach involving local thermal and chemical (for strangeness) equilibrium.

UrQMD is a microscopic many body approach to  $p+p$ ,  $p+A$  and  $A+A$  interactions at relativistic energies and is based on the covariant propagation of color strings, constituent quarks and diquarks accompanied by mesonic and baryonic degrees of freedom. The model includes rescattering of particles, the excitation and fragmentation of color strings and the formation and decay of hadronic resonances. Detailed information about the latest version of the UrQMD model can be found in [23]. We contrast this binary collision ansatz with a micro+macro hybrid approach with an embedded three-dimensional ideal relativistic one fluid evolution for the hot and dense stage of the reaction.

In the hybrid model, UrQMD serves to calculate the initial state of a heavy ion collision for the hydrodynamical evolution to account for the non-equilibrium effects in the very early stage of the collision. The coupling between the UrQMD initial state and the hydrodynamical evolution proceeds when the two Lorentz-contracted nuclei have passed through each other, i.e.  $t_{start} = 2R/\sqrt{\gamma^2 - 1}$  [25], with  $R$  being the radius of the initial nucleus and  $\gamma$  being the Lorentz factor.

The full (3+1) dimensional hydrodynamic evolution proceeds employing the SHASTA algorithm [26, 27]. To calculate the pressure, temperature and chemical potential corresponding to the energy and the baryon number densities an equation of state is needed as additional input. For the present comparison we restrict ourselves to a hadron gas equation of state which includes the same degrees of freedom as in UrQMD. The transition from the hydrodynamic phase to the Boltzmann dynamics when the system is sufficiently diluted takes place when the energy density  $\epsilon$  of a transverse slice of cells drops below five times the ground state energy density  $\epsilon_0$ . This gradual transitive procedure provides a reasonable approximation to an iso-eigentime criterion and has been applied successfully in [28, 29]. This switching criterion corresponds to a  $T-\mu_B$ -configuration where the chemical freeze-out is expected, approximately at  $T = 170$  MeV for  $\mu_B = 0$ . The hydrodynamic fields are then mapped to particle degrees of freedom via the Cooper-Frye equation on an isochronous hypersurface in each individual slice. For the production of strange baryons the corresponding chemical potentials  $\mu_B$  and  $\mu_S$  are taken into account. The strangeness chemical potential is adjusted in the calculation of the equation of state in such a way

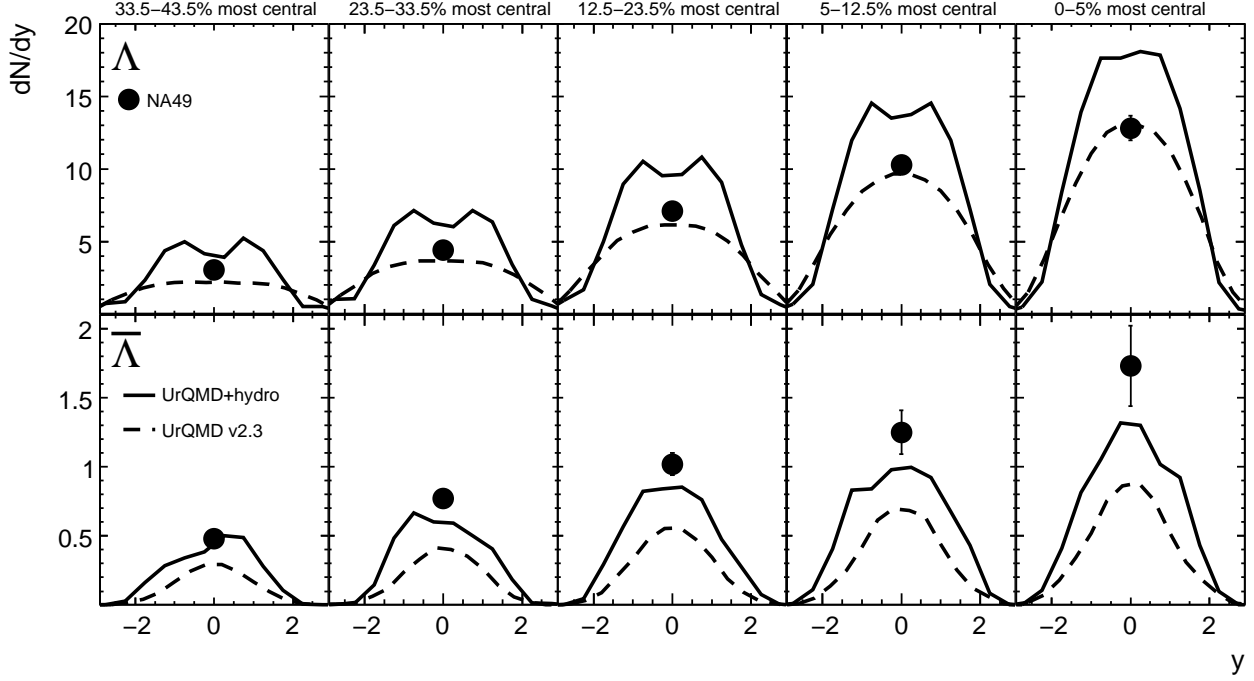


FIG. 3: The points correspond to the measured yield at midrapidity ( $|y| \leq 0.5$ ) for  $\Lambda$  (top) and  $\bar{\Lambda}$  (bottom) from NA49 [35, 36] measured for different centralities in Pb+Pb collisions at 158A GeV. The solid line represents calculations with UrQMD+hydro and the dashed line with UrQMD.

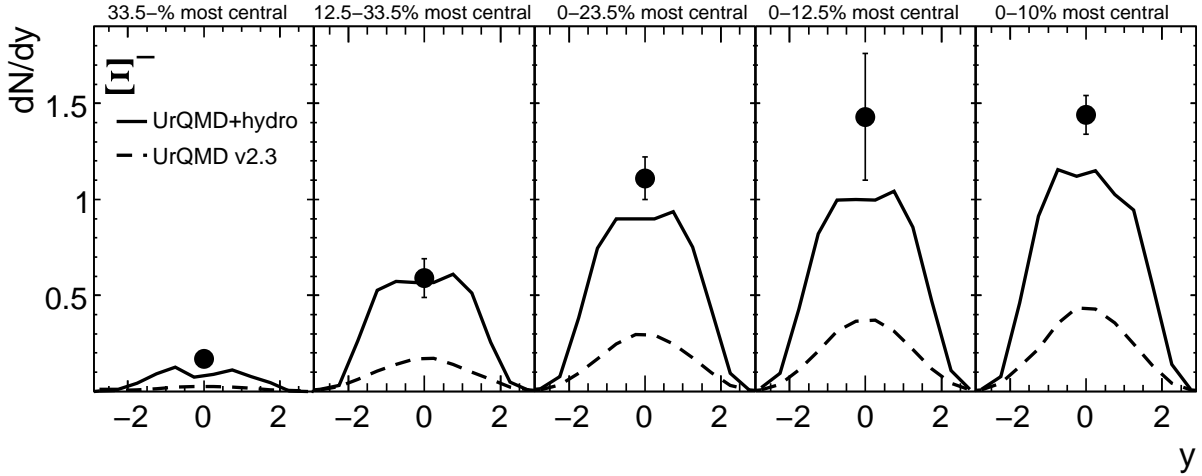


FIG. 4: The points correspond to the measured yield at midrapidity ( $|y| \leq 0.5$ ) for  $\Xi^-$  from NA49 [34, 35, 36] measured for different centralities in Pb+Pb collisions at 158A GeV. The solid line represents calculations with UrQMD+hydro and the dashed line with UrQMD.

that the net-strangeness vanishes locally. At the end of the hydrodynamic evolution the particle vector information is transferred back to the UrQMD model. Let us stress again that the present hybrid approach uses only a free hadron gas equation of state and has no phase transition included. More details about this approach including multiplicities and spectra for nonstrange particles can

be found in [24]. For a general comparison to similar approaches the reader is referred to [30, 31, 32, 33].

In the next Sections we show results from UrQMD and the hybrid approach (UrQMD+hydro). We compare these results to the measured total particle yields [43] and the abundances at midrapidity from the NA49 and NA57 experiments on Pb+Pb collisions. Furthermore, we com-

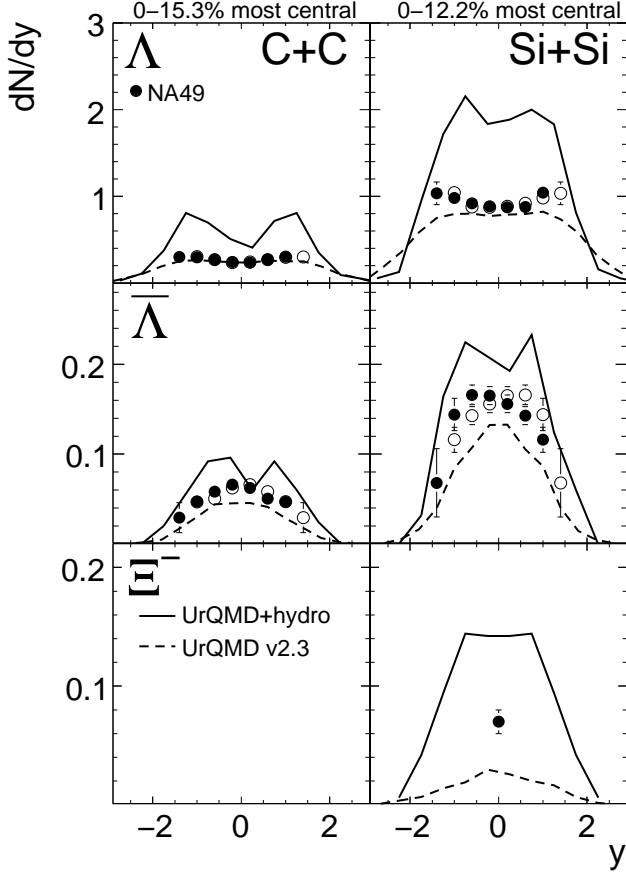


FIG. 5: The rapidity spectra of  $\Lambda$ ,  $\bar{\Lambda}$  and  $\Xi^-$  produced in central C+C (left) and Si+Si (right) collisions at 158A GeV. The closed symbols indicate measured points, open points are reflected with respect to midrapidity. The solid line represents calculations with UrQMD+hydro and the dashed line with UrQMD.

pare the model predictions to the measured  $\Lambda$ ,  $\bar{\Lambda}$  and  $\Xi^-$  rapidity spectra in central C+C and Si+Si collisions from the NA49 collaboration at 158A GeV. In addition, we present predictions from UrQMD and UrQMD+hydro for the centrality dependence of  $\Lambda$ ,  $\bar{\Lambda}$  and  $\Xi^-$  rapidity spectra at  $E_{\text{lab}} = 40A$  GeV and  $E_{\text{lab}} = 158A$  GeV and compare these to the measured yields at midrapidity ( $|y| \leq 0.5$ ).

Fig. 1 and Fig. 2 show the rapidity spectra for  $\Lambda$ ,  $\bar{\Lambda}$  and  $\Xi^-$  at  $E_{\text{lab}} = 40A$  GeV predicted from UrQMD (dashed line) and UrQMD+hydro (solid line) for different centrality bins. Data are shown as full circles [34, 35, 36] [44]. UrQMD predicts a lower multiplicity compared to the hybrid approach. This can be understood, because at the transition from the hydrodynamic evolution to the hadronic cascade the particles are produced according to thermal distributions. In this manner, it is much easier to produce especially multistrange hyperons than via resonance and string excitation. The hadronic cross sections of strange baryons are small, so they do not get

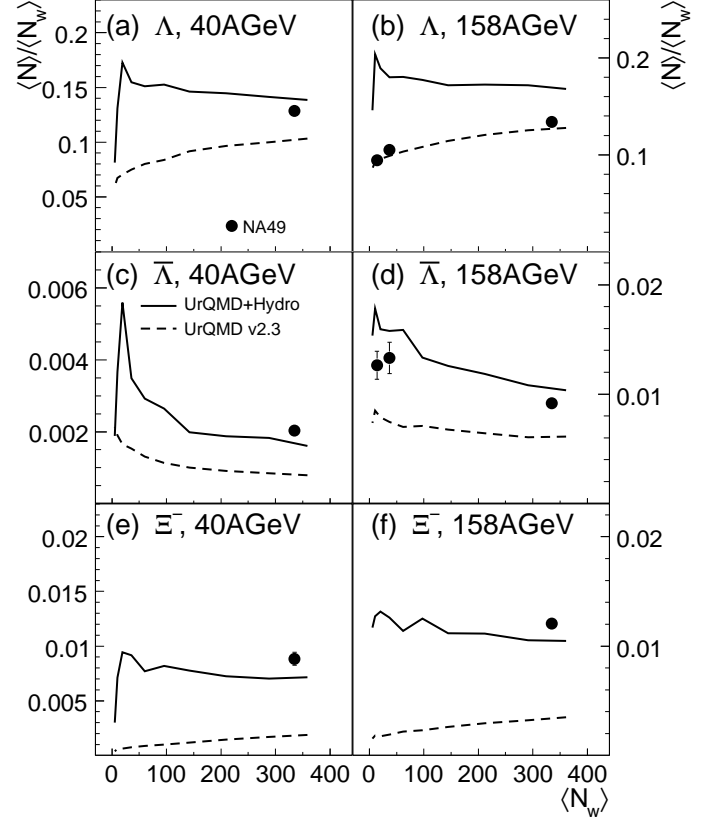


FIG. 6: The points correspond to the measured total yield by NA49 at 40A (left) and 158A GeV (right) [34, 35, 36, 37, 38, 39]. The solid line represents calculations with UrQMD+hydro and the dashed line with UrQMD.

reequilibrated during the hadronic expansion phase once they are produced. The only exception are the  $\bar{\Lambda}$ 's which get absorbed even during the late stage of the evolution. The  $\Lambda$  production in the pure transport approach is in a reasonable agreement with the experimental data because their production threshold is not as high as for the other hyperons because they are likely to be produced in nucleon-nucleon collisions in association with a kaon (see Table I). Therefore, the  $\Lambda$ 's reflect the initial baryon stopping and the rapidity distribution of the net baryon number and should not be regarded as a part of the produced thermal system. The assumption of chemical equilibrium leads to an enhanced  $\bar{\Lambda}$  and  $\Xi$  production in good agreement to the experimental data. The same trend is also visible at  $E_{\text{lab}} = 158A$  GeV (see Fig. 3 and Fig. 4). However, here the difference between the  $\bar{\Lambda}$  calculated in UrQMD (dashed line) and UrQMD+hydro (solid line) is smaller than at  $E_{\text{lab}} = 40A$  GeV.

To explore the applicability limit of the hybrid model in terms of collision volume, Fig. 5 shows the rapidity spectra of  $\Lambda$  and  $\bar{\Lambda}$  for central C+C and Si+Si collisions at 158A GeV measured by the NA49 collaboration [37, 38]. It is visible that for such small systems UrQMD (dashed line) describes the data better than

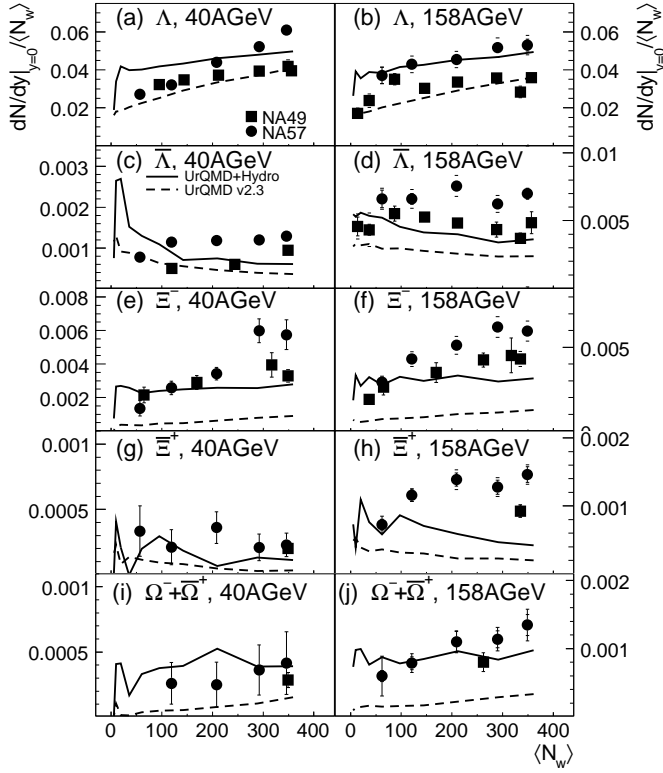


FIG. 7: Centrality dependence of the (anti-) hyperon yields at midrapidity ( $|y| \leq 0.5$ ) at 40A (left) and 158A GeV (right) measured by NA49 (squares) [34, 35, 36, 37, 38, 39] and NA57 (circles) [40, 41, 42]. The solid line represents calculations with UrQMD+hydro and the dashed line with UrQMD.

UrQMD+hydro (solid line). The reason for this observation is that the limited system size does not allow for a full thermalization in C+C and Si+Si interactions like in the case of Pb+Pb collisions. This indicates that up to Si+Si reactions, thermalization can not be achieved and the system is merely a (non-) trivial convolution of elementary baryon-baryon (and in smaller parts meson-baryon) interactions. From this, we also conclude that the possibility of a phase transition is reduced in such small systems.

Let us next focus on a detailed study of the centrality dependence of strange baryons in Pb+Pb reactions. Fig. 6 depicts the predictions of the centrality dependence of the total yield of  $\Lambda$ ,  $\bar{\Lambda}$  and  $\Xi^-$  at  $E_{\text{lab}} = 40A$  GeV and  $E_{\text{lab}} = 158A$  GeV. One clearly observes that for central collisions the assumption of a thermalized system leads to a suitable description of the strangeness production within the hybrid model calculation.

The centrality and system size dependence of (anti-) hyperon production at 40A and 158A GeV at midrapidity ( $|y| \leq 0.5$ ) is shown in Fig. 7 measured by the NA49 [34, 35, 36, 39] and NA57 [40, 41, 42] collaborations. A discrepancy between both experiments is observed. However, for a qualitative interpretation, the present data are sufficient and we will therefore refrain

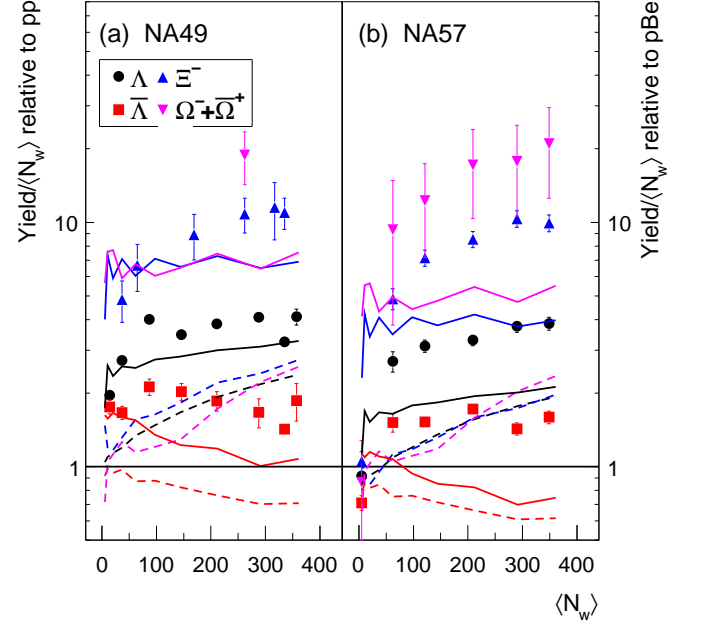


FIG. 8: (color online) Hyperon enhancement as a function of  $N_w$  at 158A GeV measured from NA49 (right) and NA57 (left). Note NA57 uses p+Be instead of p+p as baseline.

from speculations on the origin of the experimental inconsistencies. The dashed line represents calculations with UrQMD and the solid line indicates predictions from UrQMD+hydro simulations. The pure transport approach describes the data in very peripheral collisions quite well. The reason why UrQMD works for very peripheral Pb+Pb or small systems like C+C/Si+Si is that the system is not in equilibrium as discussed above. Moving to more central Pb+Pb collisions it is visible that the thermal production of strange quarks is in much better agreement with the measured data than obtained in the binary collision prescription. Especially for multistrange hyperons it is visible that the production via independent strings and resonance excitations is not sufficient to explain the experimentally measured yields. From this, we conclude that the assumption of thermalization alone allows to explain a major part of the strangeness enhancement in central collisions of massive nuclei. However, firm conclusion on the formation of a QGP can not be drawn from this. For peripheral reactions or small collision systems a description by subsequent hadronic interactions is favoured.

Finally, the hyperon enhancement as a function of the number of wounded nucleons,  $\langle N_w \rangle$ , at 158A GeV measured by NA49 (a) [34, 35, 36, 37, 38, 39] and NA57 (b) [40, 41, 42] is shown in Fig. 8. The strangeness enhancement is defined as the yield per participant in Pb+Pb collisions normalized to the yield per participant in p+p or p+Be interactions:

$$E = \left( \frac{Yield}{N_w} \right)_{A+A} / \left( \frac{Yield}{N_w} \right)_{p+p/p+Be}, \quad (1)$$

The hybrid calculation leads to a mostly centrality independent result because the system at the freeze-out transition is described by grand-canonical distributions. For the  $\bar{\Lambda}$  the absorption during the hadronic rescattering stage is reflected in the centrality dependence.

A clear hierarchy is visible depending on the strangeness content. The shape of the centrality dependence is changing from a decreasing distribution for  $\bar{\Lambda}$  to an increasing shape for  $\Lambda$ ,  $\Xi^-$  and  $\Omega^- + \bar{\Omega}^+$  with an enhancement for  $\Omega^- + \bar{\Omega}^+$  of approximately 10. UrQMD clearly underpredicts the effects, in all cases.

In this paper we presented predictions for the system size and centrality dependence of strange (anti-) hyperons at 40A and 158A GeV from the Ultra-relativistic Quantum Molecular Dynamics model (UrQMD) and a hybrid model that incorporates a (3+1) dimensional hydrodynamic evolution into the UrQMD transport approach. We started by showing the predicted centrality dependence of the rapidity spectra for  $\Lambda$ ,  $\bar{\Lambda}$  and  $\Xi^-$  in

Pb+Pb collisions at  $E_{lab} = 40A$  GeV and  $E_{lab} = 158A$  GeV where it was visible that due to the thermal production of strangeness in the UrQMD+hydro model a higher hyperon yield is generated. Compared to Pb+Pb collisions the system seemed not fully thermalized in C+C and Si+Si collisions and therefore UrQMD provided a better description of the measured rapidity spectra. The conclusion is that thermalization is only reached for central Pb+Pb collisions. The production of strange (anti-) hyperons in smaller systems like C+C and Si+Si can be described with a binary scattering transport approach like UrQMD.

This work was supported by the Hessian LOEWE initiative through HIC for FAIR. We are grateful to the Center for Scientific Computing (CSC) at Frankfurt for the computing resources. H. Petersen gratefully acknowledges financial support by the Deutsche Telekom Stiftung and support from the Helmholtz Research School on Quark Matter Studies. T. Schuster gratefully acknowledges support from the Helmholtz Research School on Quark Matter Studies. This work was supported by GSI, BMBF and DESY. The authors would also like to thank C. Blume.

- 
- [1] S. A. Bass, M. Gyulassy, H. Stoecker and W. Greiner, J. Phys. G **25**, R1 (1999).
  - [2] X. N. Wang, Phys. Rept. **280**, 287 (1997).
  - [3] J. W. Harris and B. Muller, Ann. Rev. Nucl. Part. Sci. **46**, 71 (1996).
  - [4] J. Rafelski and B. Muller, Phys. Rev. Lett. **48**, 1066 (1982) [Erratum-ibid. **56**, 2334 (1986)].
  - [5] P. Koch, B. Muller and J. Rafelski, Phys. Rept. **142**, 167 (1986).
  - [6] H. J. Drescher, J. Aichelin and K. Werner, Phys. Rev. D **65**, 057501 (2002).
  - [7] M. Bleicher *et al.*, Phys. Rev. Lett. **88**, 202501 (2002).
  - [8] S. E. Vance and M. Gyulassy, Phys. Rev. Lett. **83**, 1735 (1999).
  - [9] J. S. Schwinger, Phys. Rev. **82**, 664 (1951).
  - [10] T. S. Biro, H. B. Nielsen and J. Knoll, Nucl. Phys. B **245** (1984) 449.
  - [11] J. Knoll, Z. Phys. C **38**, 187 (1988).
  - [12] H. Sorge, M. Berenguer, H. Stoecker and W. Greiner, Phys. Lett. B **289**, 6 (1992); M. Bleicher, W. Greiner, H. Stoecker and N. Xu, Phys. Rev. C **62**, 061901 (2000); S. Soff *et al.*, Phys. Lett. B **471**, 89 (1999).
  - [13] N. S. Amelin, M. A. Braun and C. Pajares, Phys. Lett. B **306**, 312 (1993).
  - [14] C. Greiner and S. Leupold, J. Phys. G **27**, L95 (2001).
  - [15] W. Cassing, Nucl. Phys. A **700**, 618 (2002).
  - [16] R. Rapp and E. V. Shuryak, Phys. Rev. Lett. **86**, 2980 (2001).
  - [17] P. Braun-Munzinger, J. Stachel and C. Wetterich, Phys. Lett. B **596**, 61 (2004).
  - [18] J. Noronha-Hostler, C. Greiner and I. A. Shovkovy, Phys. Rev. Lett. **100**, 252301 (2008).
  - [19] K. Redlich and A. Tounsi, Eur. Phys. J. C **24**, 589 (2002).
  - [20] C. Hohné, F. Puhlhofer and R. Stock, Phys. Lett. B **640**, 96 (2006).
  - [21] M. Bleicher *et al.*, J. Phys. G **25**, 1859 (1999).
  - [22] S. A. Bass *et al.*, Prog. Part. Nucl. Phys. **41**, 255 (1998).
  - [23] H. Petersen, M. Bleicher, S. A. Bass and H. Stöcker, arXiv:0805.0567 [hep-ph].
  - [24] H. Petersen, J. Steinheimer, G. Burau, M. Bleicher and H. Stoecker, Phys. Rev. C **78**, 044901 (2008).
  - [25] J. Steinheimer, M. Bleicher, H. Petersen, S. Schramm, H. Stoecker and D. Zschesche, Phys. Rev. C **77**, 034901 (2008).
  - [26] D. H. Rischke, S. Bernard and J. A. Maruhn, Nucl. Phys. A **595**, 346 (1995).
  - [27] D. H. Rischke, Y. Pursun and J. A. Maruhn, Nucl. Phys. A **595**, 383 (1995) [Erratum-ibid. A **596**, 717 (1996)].
  - [28] H. Petersen and M. Bleicher, of the arXiv:0901.3821 [nucl-th].
  - [29] Q. f. Li, J. Steinheimer, H. Petersen, M. Bleicher and H. Stoecker, arXiv:0812.0375 [nucl-th].
  - [30] A. Dumitru, S. A. Bass, M. Bleicher, H. Stoecker and W. Greiner, Phys. Lett. B **460**, 411 (1999).
  - [31] D. Teaney, J. Lauret and E. V. Shuryak, arXiv:nucl-th/0110037.
  - [32] C. Nonaka and S. A. Bass, Phys. Rev. C **75**, 014902 (2007).
  - [33] Y. Hama, R. P. G. Andrade, F. Grassi, W. L. Qian and T. Kodama, arXiv:0901.2849 [hep-ph].
  - [34] C. Alt *et al.* [NA49 Collaboration], Phys. Rev. C **78**, 034918 (2008).
  - [35] C. Blume [NA49 Collaboration], J. Phys. G **34**, S951 (2007).
  - [36] M. K. Mitrovski *et al.* [NA49 Collaboration], J. Phys. G **32** (2006) S43.

- [37] C. Alt *et al.* [NA49 Collaboration], Phys. Rev. Lett. **94**, 052301 (2005).
- [38] I. Kraus, PhD thesis, Johann Wolfgang Goethe-Universität Frankfurt (2004).
- [39] C. Alt *et al.* [NA49 Collaboration], Phys. Rev. Lett. **94**, 192301 (2005).
- [40] F. Antinori *et al.* [NA57 Collaboration], J. Phys. G **32**, 427 (2006).
- [41] F. Antinori *et al.* [NA57 Collaboration], Phys. Lett. B **595**, 68 (2004).
- [42] <http://wa97.web.cern.ch/WA97/yields.html>
- [43] Note that only the NA49 has the acceptance to measure the total multiplicity.
- [44] We extrapolate the midrapidity yields of the NA49 data for every centrality class of  $\bar{\Lambda}$  by using an exponential fit.